

RESEARCH ARTICLE | SEPTEMBER 09 2025

RNA gradients can guide condensates toward promoters: Implications for enhancer–promoter contacts and condensate-promoter kissing

Special Collection: [Chromatin Structure and Dynamics: Recent Advancements](#)

David Goh  ; Deepti Kannan  ; Pradeep Natarajan  ; Andriy Goychuk   ; Arup K. Chakraborty 



J. Chem. Phys. 163, 104905 (2025)

<https://doi.org/10.1063/5.0277838>

 [CHORUS](#)



View
Online



Export
Citation

Articles You May Be Interested In

Surface properties of the polarizable Baranyai-Kiss water model

J. Chem. Phys. (March 2012)

Footprints of loop extrusion in statistics of intra-chromosomal distances: An analytically solvable model

J. Chem. Phys. (March 2024)

Estimating random close packing in polydisperse and bidisperse hard spheres via an equilibrium model of crowding

J. Chem. Phys. (January 2023)

RNA gradients can guide condensates toward promoters: Implications for enhancer-promoter contacts and condensate-promoter kissing

Cite as: J. Chem. Phys. 163, 104905 (2025); doi: 10.1063/5.0277838

Submitted: 26 April 2025 • Accepted: 25 July 2025 •

Published Online: 9 September 2025



David Goh,^{1,2,a)} Deepti Kannan,³ Pradeep Natarajan,¹ Andriy Goychuk,^{4,b,c)} and Arup K. Chakraborty^{1,3,4,5,6,b)}

AFFILIATIONS

¹ Department of Chemical Engineering, Massachusetts Institute of Technology, Cambridge, Massachusetts 02139, USA

² Department of Chemical Engineering, Imperial College London, London SW7 2AZ, United Kingdom

³ Department of Physics, Massachusetts Institute of Technology, Cambridge, Massachusetts 02139, USA

⁴ Institute for Medical Engineering and Science, Massachusetts Institute of Technology, Cambridge, Massachusetts 02139, USA

⁵ Department of Chemistry, Massachusetts Institute of Technology, Cambridge, Massachusetts 02139, USA

⁶ Ragon Institute of MGH, MIT, and Harvard, Cambridge, Massachusetts 02139, USA

Note: This paper is part of the JCP Special Topic on Chromatin Structure and Dynamics: Recent Advancements.

^{a)}**Present address:** Institute for Medical Engineering and Science, Massachusetts Institute of Technology, Cambridge, Massachusetts 02139, USA.

^{b)}**Authors to whom correspondence should be addressed:** andriy@goychuk.me and arupc@mit.edu

^{c)}**Present address:** Helmholtz-Center for Infection Research, 38124 Braunschweig, Germany.

ABSTRACT

We study how protein condensates respond to a site of active RNA transcription (i.e., a gene promoter) due to electrostatic protein–RNA interactions. Our results indicate that condensates can show directed motion toward the promoter, driven by gradients in the RNA concentration. Analytical theory, consistent with simulations, predicts that the droplet velocity has a non-monotonic dependence on the distance to the promoter. We explore the consequences of this gradient-sensing mechanism for enhancer–promoter (E–P) communication using polymer simulations of the intervening chromatin chain. Directed motion of enhancer-bound condensates can, together with loop extrusion by cohesin, collaboratively increase the enhancer–promoter contact probability. Finally, we investigate under which conditions condensates can exhibit oscillations in their morphology and in the distance to the promoter. Oscillatory dynamics are caused by a delayed response of transcription to condensate-promoter contact and negative feedback from the accumulation of RNA at the promoter, which results in charge repulsion.

© 2025 Author(s). All article content, except where otherwise noted, is licensed under a Creative Commons Attribution (CC BY) license (<https://creativecommons.org/licenses/by/4.0/>). <https://doi.org/10.1063/5.0277838>

I. INTRODUCTION

Biomolecular condensates compartmentalize different biochemical reactions by enriching the local concentrations of specific reactants and enzymes.^{1,2} Condensates are believed to form through liquid–liquid phase separation, which is driven by a network of weak multivalent interactions among proteins.^{1–4} The properties of condensates can be modulated by interactions between proteins and nucleic acids, such as DNA and RNA.^{5–12} When molecular interactions are coupled with irreversible chemical

reactions, biomolecular condensates can exhibit a variety of rich phenomena not present in thermal equilibrium.¹³ Past theoretical studies have investigated how reactions can lead to nonequilibrium phenomena such as arrested coarsening,^{14–22} droplet division and anti-coarsening,^{18,20,21,23} self-propulsion,^{20,24–26} and directed motion.^{27–29}

Coupling phase separation with irreversible chemical reactions may be a generic feature of intracellular dynamics. For example, transcriptional condensates are composed of proteins required for RNA transcription, including RNA polymerase II, transcription

factors (TFs), and coactivators.^{5,30–35} These proteins have positively charged regions, which interact electrostatically with the freshly transcribed negatively charged RNA.¹² These interactions were shown to give rise to a reentrant phase transition, where at low RNA concentrations, attractive interactions recruit proteins into the condensate, whereas at high RNA levels, repulsive interactions expel proteins from the condensate.^{10–12} As a result, an excess of transcribed RNA can dissolve transcriptional condensates, providing a negative feedback loop for transcription.¹² When transcription is spatially localized to active genes, computer simulations further show that condensates can move toward these genes and adopt nonequilibrium steady state morphologies, such as vacuoles and aspherical shapes.²⁹ These simulation results are corroborated by experimental studies that have observed nuclear condensates showing directed motion^{36–39} and adopting aspherical morphologies.⁴⁰

Past theoretical studies have characterized the motion of condensates due to externally imposed^{27,28} or self-generated concentration gradients.^{20,26} In both cases, droplet motion is driven by a chemical potential gradient across the droplet, which creates a net flux of proteins.²⁶ Motivated by these theoretical results and experimental observations of droplet motion *in vitro*,^{41,42} we asked if this *gradient-sensing* mechanism could explain the localization of transcriptional condensates toward active gene promoters, which generate RNA concentration gradients via transcription. Building on the self-consistent sharp interface theory developed in Ref. 26, we analytically calculate the velocity of transcriptional condensates as they flow toward gene promoters and demonstrate its agreement with simulations. We then explore the consequences of this directed motion for gene regulation, focusing on the interactions between enhancers, condensates, and promoters.

Transcriptional condensates form at chromatin loci enriched with TF-DNA binding sites, such as super-enhancers,^{5,30,31,43} and are believed to remain bound to chromatin.³² Enhancers regulate gene expression by interacting with their cognate promoters,⁴⁴ but the mechanisms that bring enhancers and promoters into spatial proximity remain unclear.⁴⁵ Cohesin can increase the contact frequency between enhancers and promoters by extruding loops,⁴⁶ yet, depleting cohesin does not fully abrogate all enhancer-promoter contacts.^{47–54} Transcriptional condensates are speculated to act as a bridge between the enhancer and the promoter, a mechanism that is known as the “action-at-a-distance” model.^{45,55,56} As a result, the condensate enriches the concentration of transcriptional proteins around the promoter, which may drive higher rates of transcription.^{30,34,57} However, the role of condensates in bringing the enhancer and promoter into proximity, if any, remains unexplored.⁵⁸

Here, we propose that condensate motion in response to an RNA concentration gradient results in a non-reciprocal interaction that attracts enhancer-bound condensates toward promoters, but not vice versa. Brownian dynamics simulations of a polymer model of chromatin show that this non-reciprocal interaction increases the enhancer-promoter contact probability. We hypothesize, supported by simulations, that gradient-sensing can cooperate with loop extrusion to robustly give rise to enhancer-promoter contacts over different length scales.⁵⁹

We next shift our focus to more dynamic models of condensate-promoter communication. In particular, live-cell

imaging studies have observed transient and dynamic kissing events between condensates and gene promoters reminiscent of oscillations.^{32,35} Inspired by these observations, we wondered under what conditions our model could admit oscillations in condensate-promoter proximity. In the cell, the transcription machinery enriched within transcriptional condensates first assembles into a preinitiation complex. RNA polymerase II then stalls near the promoter during promoter-proximal pausing before finally proceeding to the productive elongation of RNA.^{60–62} These processes can give rise to an effective time delay between condensate-promoter contact and transcription. We demonstrate that coupling such delays with the negative feedback from RNA accumulation^{10–12} can produce oscillatory dynamics. Finally, we discuss the implications of our results for dynamic models of enhancer-promoter communication.

II. MODEL

Based on prior studies,^{12,29,63} we consider a phase field model where a conserved species of transcriptional proteins, with concentration $c(\mathbf{x}, t)$, regulates the production of a non-conserved species of nascent RNA, with concentration $m(\mathbf{x}, t)$. We assume that the minimization of the following free energy of protein–protein interactions results in their spontaneous phase separation at equilibrium,

$$\mathcal{F}_{cc}(c) = \int d^d r \left[\frac{\alpha}{4} (c - \bar{c})^4 + \frac{\beta}{2} (c - \bar{c})^2 + \frac{\kappa}{2} |\nabla c|^2 \right], \quad (1)$$

where \bar{c} is the critical point. The parameter $\beta < 0$ sets the difference between the concentrations of the protein-rich and the protein-poor binodal points, $c_{\pm}^* = \bar{c} \pm \sqrt{-\beta/\alpha}$. The surface tension, which acts to minimize the condensate interface, is parameterized by $\kappa > 0$.

Electrostatic interactions between positively charged proteins and negatively charged RNA lead to a reentrant phase transition driven by a balance of charges, which is known as complex coacervation.^{10–12} This phenomenon can be captured using a phenomenological free energy of the form

$$\mathcal{F}_{cm}(c, m) = \int d^d r \left[\chi cm + \frac{\gamma}{2} c^2 m^2 \right], \quad (2)$$

where attractive interactions ($\chi < 0$) dominate at low RNA concentrations, and repulsive interactions ($\gamma > 0$) dominate at high RNA concentrations. Although symmetry arguments do not preclude terms of the form mc^2 and cm^2 in the above-mentioned Landau–Ginzburg expansion, it was previously shown that these terms are not necessary for the system to show a reentrant phase transition.¹² In Secs. III and IV, we first focus on the regime of low RNA concentrations and, therefore, only consider the pairwise interaction term (i.e., we make the approximation $\gamma \approx 0$). In Sec. V, we explore the effects of the higher order repulsive RNA–protein interactions on the droplet dynamics. Altogether, the thermodynamics of the protein–RNA system is characterized by the free energy functional,

$$\mathcal{F} = \mathcal{F}_{cc}(c) + \mathcal{F}_{cm}(c, m). \quad (3)$$

Since protein turnover is slow compared to nascent RNA transcription, we assume the amount of protein to be conserved. Protein mass is redistributed by gradient flows, minimizing the net free energy,

$$\begin{aligned} \partial_t c &= -\nabla \cdot J, \\ J &= -M_c(\nabla \mu_{cc} + \nabla \mu_{cm}), \end{aligned} \quad (4)$$

where we have separated the contributions to the current due to protein–protein interactions alone, $\mu_{cc} = \delta \mathcal{F}_{cc}/\delta c$, and due to protein–RNA interactions, $\mu_{cm} = \delta \mathcal{F}_{cm}/\delta c$. The protein mobility M_c is assumed to be constant for consistency with prior studies.^{12,29,63}

RNA is actively produced in regions with high concentrations of the transcription machinery, under consumption of nucleoside triphosphates (NTPs). Hence, in our model, RNA is produced at a rate $k_p c > 0$ spatially localized around a point on the gene locus. The dynamics are thus governed by a reaction–diffusion equation

$$\partial_t m = D_m \nabla^2 m + k_p \exp\left(-\frac{|\mathbf{r} - \mathbf{r}_p|^2}{2\sigma_p^2}\right) c - k_d m, \quad (5)$$

where D_m is the diffusion coefficient of nascent RNA, and k_d is the rate at which nascent RNA is modified into a form that ablates its interactions with transcriptional proteins. Since the DNA from which the RNA is transcribed has a Gaussian end-to-end distribution, the variance σ_p^2 of the spatial production rate is a proxy

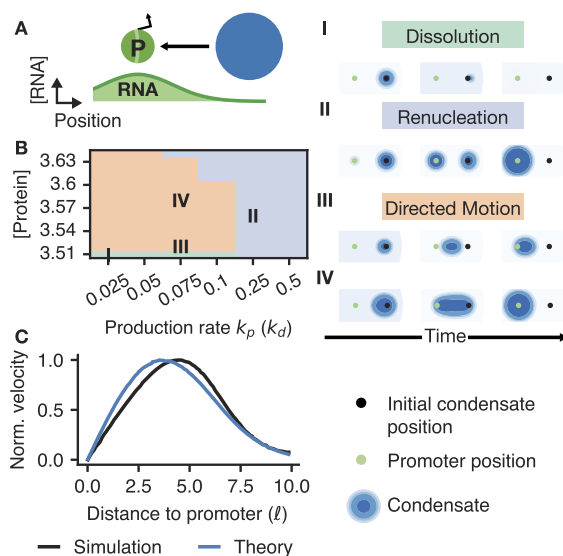


FIG. 1. Condensates can sense RNA gradients and move toward gene promoters. (a) Transcription at the gene promoter produces RNA, which diffuses and degrades, resulting in an RNA concentration gradient. The promoter is indicated by the green circle, the condensate by the blue circle, and the RNA concentration gradient by the green curve. (b) Condensates can dissolve (I), dissolve and renucleate at the promoter (II), or exhibit directed motion toward the promoter (III, IV) depending on the RNA production rate k_p (in units of the degradation rate k_d) and the total protein concentration, which we control by varying the initial concentration of proteins outside the droplet $c_-(t=0)$. Droplet elongation is enhanced at higher protein concentrations (IV). Simulation parameters: $\alpha = 1$, $\beta = -0.25$, $\kappa = 0.05$, $\chi = -0.1$, $\gamma = 0$, $M_c = 1$, $D_m = 1$, $\sigma_p = 2.5$, $k_d = 1$, $c_+(t=0) = 5.5$, $m(\mathbf{r}, t=0) = 0$, $r(t=0) = 10$, and $R(t=0) = 2$. (c) Droplet velocity, normalized by the maximum value, is non-monotonic in the distance between the droplet center of mass and the promoter (reported in units of the RNA diffusion length, $\ell = \sqrt{D_m/k_d}$). Theoretical predictions show that directed motion is driven by RNA gradients [Eq. (9)]. Simulation parameters specific to panel (c): $k_p = 0.08$ and $c_-(t=0) = 3.53$.

for the length of the gene. Alternatively, the Gaussian localization function can be interpreted as the density of promoters in a cluster of genes.²⁹ We simulate the coupled protein and RNA dynamics with the promoter located at the origin ($\mathbf{r}_p = \mathbf{0}$). We employ finite volume simulations using a circular mesh with no-flux boundary conditions for both species. We set the length scale to be the diffusion length of RNA, $\ell = \sqrt{D_m/k_d}$, and the time scale to be the inverse of the RNA degradation rate, $1/k_d$ (supplementary material, Sec. SI).

III. RNA GRADIENT SENSING CAUSES DIRECTED MOTION OF CONDENSATES TOWARDS GENE PROMOTERS

We first investigate how a condensate responds to RNA concentration gradients generated by transcription at an active promoter [Fig. 1(a)] using simulations in two dimensions and theoretical analysis of the dynamics in Eqs. (4) and (5). In this section, we consider a regime in which RNA concentrations are low, such that RNA–protein interactions are mainly attractive. That is, we only include the pairwise interaction term in Eq. (2), χcm . In Sec. V, we will also study the more general scenario where RNA concentrations can be high. In our phase field simulations, we initialize a circular droplet of radius $R(t=0) = 2$ with initial dense phase concentration $c_+(t=0) = 5.5$ at a fixed initial distance $r(t=0) = 10$ between the condensate center-of-mass and the promoter. We set the initial RNA concentration to $m(\mathbf{r}, t=0) = 0$ and simulate the protein and RNA dynamics by solving Eqs. (4) and (5) using finite-volume methods.

We find that the dynamics of the droplet are most influenced by the RNA production rate and the total amount of protein in the system, which we control by varying the initial concentration of proteins outside the droplet [Fig. 1(b)]. For average protein concentrations close to the protein-poor binodal point ($c_-^* = 3.5$), the nucleated droplet dissolves because a homogeneous light phase admits a lower free energy than a two-phase system [Fig. 1(b)(I)]. At high RNA production rates, the protein–RNA attraction is strong enough to dissolve the first condensate and nucleate another at the promoter [Fig. 1(b)(II)]. At lower RNA production rates, if the protein concentration is not too low, the droplet instead flows toward the RNA source [Figs. 1(b)(III) and 1(b)(IV)]. The droplet elongates as it flows, as has been observed in experiments on the directed motion of nuclear speckles.³⁹ Droplet elongation is enhanced at higher protein concentrations [Fig. 1(b)(IV)] and lower surface tensions controlled by κ (Figs. S2 and S3).

To further investigate what drives droplet flow, we quantify the flow velocity analytically with the method outlined in Ref. 26. First, we assume the droplet flows with a constant velocity (i.e., steady motion) and, therefore, seek a traveling-wave solution $c(\mathbf{x} - vt) \equiv c(z)$ to the continuity equation

$$-\mathbf{v} \cdot \nabla c(z) = \nabla \cdot [M_c(\nabla \mu_{cc} + \nabla \mu_{cm})]. \quad (6)$$

To analyze Eq. (6) analytically, we take the sharp interface limit, meaning the interface width $w = \sqrt{2\kappa/\beta}$ is smaller than all other length scales relevant to the dynamics. Mathematically, we simultaneously take the limits $\alpha \rightarrow \infty$ and $\beta \rightarrow \infty$, which maintains finite dense and light phase concentrations, $c_{\pm} = \bar{c} \pm \sqrt{-\beta/\alpha}$, while implying an infinite effective surface tension and, therefore, a round

droplet shape.²⁶ We thus consider a piecewise constant protein concentration profile $c(z)$ where the concentration within the droplet is assumed to be equivalent to the protein-rich binodal, $c_+^* = 4.5$, and the concentration outside the droplet is set to the protein-poor binodal, $c_-^* = 3.5$.

Having imposed a droplet concentration profile, we temporarily assume knowledge of the droplet velocity \mathbf{v} and derive a constraint on $\mu_{cc}(z|\mathbf{v})$ that adiabatically maintains a piecewise constant protein concentration field. In Eq. (6), the effective force due to protein–RNA interactions, $-\nabla\mu_{cm}$, breaks energy conservation because RNA is continuously produced and degraded. In contrast, the current of proteins $\mathbf{j} = c(z)\mathbf{v}$ in the presence of the purely thermodynamic force $-\nabla\mu_{cc}$ should not dissipate power,²⁶

$$\partial_t \mathcal{F}_{cc}[c] = \mathbf{v} \cdot \int_D d^d z \ c(z) \nabla \mu_{cc} = 0. \quad (7)$$

Because μ_{cc} far from the droplet is uniform, following Ref. 26, one can show that Eq. (7) reduces to the following thermodynamic consistency condition involving an integral over the domain D of the droplet, $|z| \leq R$,

$$\int_D d^d z \ \hat{\mathbf{e}}_v \cdot \nabla \mu_{cc} = 0. \quad (8)$$

The condition in Eq. (8) implies that the effective force due to protein–protein interactions alone must be symmetric about the droplet center in the direction of flow $\hat{\mathbf{e}}_v$.

With the above-mentioned simplifications, one can first solve Eq. (6) for the unknown function $\mu_{cc}(z|\mathbf{v})$ and then use Eq. (8) to determine the droplet velocity \mathbf{v} .²⁶ For a constant mobility of the proteins, we find that in $d = 2$ or $d = 3$ dimensions (supplementary material, Sec. SIII),

$$\mathbf{v} = -\frac{dM_c\chi}{\Delta c V_D} \int_D d^d r \ \hat{\mathbf{e}}_v \cdot \nabla m(\mathbf{r}), \quad (9)$$

where $V_D \sim R^d$ is the droplet volume. Equation (9) demonstrates that the directed motion of the droplet is driven by concentration gradients in RNA. The velocity is proportional to the strength of the RNA–protein attraction χ and the protein mobility M_c but inversely proportional to the concentration difference between the dense and light phases, $\Delta c \equiv c_+^* - c_-^*$. Note that the droplet velocity is enhanced by a factor of the number of dimensions, d , compared to calculations reported in prior literature where the droplet is treated akin to a solid so that all material points within the droplet move at the same velocity.^{27,29} In essence, transport is driven both by a roughly 1D flux of proteins in the dense phase and, in addition, amplified by $d - 1$ dimensions in which droplet material is brought from the trailing edge across the light phase and into the leading edge of the droplet. Therefore, the leading edge is continuously being renucleated as the droplet moves, which also explains why the droplet velocity is inversely proportional to the strength of phase separation, Δc .

Our analytical calculation in Eq. (9) relies on the assumption of an overdamped system where the droplet adjusts its velocity instantaneously in response to the RNA concentration field. To simplify our analytical calculations, we assume that the RNA concentration field is in steady state and neglect the effect of the droplet on RNA production. We obtain the fixed RNA profile from the steady state

solution of Eq. (5) and substitute the RNA concentration gradient in Eq. (9). In our simulations, the RNA profile does change in response to droplet motion, hence leading to a feedback mechanism; we quantify the effect of a time-varying RNA field on condensate motion in supplementary material, Fig. S6. Equation (9) also assumes a fixed droplet radius; however, in simulations, the droplet radius grows with time due to coarsening and attractive interactions with the RNA, which promote incorporation of the light phase protein into the dense phase.²⁷ In the absence of an analytical expression for the droplet size and shape as a function of time, we determine its effective radius from simulations by calculating the angular average of the distance between each point along the contour of the droplet and the droplet center of mass (supplementary material).

In Fig. 1(c), we compare the velocity of droplets simulated in $d = 2$ dimensions, normalized by the maximum value, to the theoretical prediction of Eq. (9) as a function of distance from the RNA source, r . When the droplet centroid and the RNA source colocalize, the RNA concentration profile is symmetric about the droplet center, causing motion to stop. In the range $r \leq R$, the gradient in the RNA concentration profile progressively increases until it reaches a maximum at $r = R = 4$, where the leading edge of the droplet coincides with the promoter where the RNA profile has its maximum. The velocity then decays with the gradient of the RNA profile, which has a characteristic length scale that can be approximated by the sum of the standard deviation of the Gaussian production rate, σ_p , and the RNA diffusion length ℓ [cf. Eq. (S22)]. Note that if the initial distance between the condensate and the promoter is much greater than this length scale, then directed motion is so slow that it is unlikely to be observed on experimental or simulation timescales.²⁹

In our simulations, the droplet elongates as it flows; as a result, the distance at which the leading edge touches the promoter is the major axis of the ovular droplet. This axis is longer than the angular average of the droplet radius (supplementary material, Fig. S8) used in the theoretical calculation. Therefore, in simulations, the velocity peaks at a distance slightly larger than the angular-averaged droplet radius. In simulations of perfectly round droplets, the peaks of the simulation and theory curves align (supplementary material, Fig. S11).

While the shapes of the velocity vs distance curves are similar in simulations and theory, the theory underpredicts the maximum of the velocity by 29.3%. One reason for this discrepancy is that the simulations in Fig. 1(c) feature a time-varying RNA gradient that responds to droplet motion. Simulations of droplet motion in response to a fixed RNA gradient more closely match the theoretical prediction (supplementary material, Fig. S6). In addition, our theoretical calculations assume $\Delta c = 4.5 - 3.5 = 1$ is determined by the binodal points, whereas simulations show that the difference in concentration between the dense and light phases is always less than one and increases as the droplet flows toward the promoter. Accounting for both of these effects explains most of the discrepancy between simulations and theory (supplementary material, Fig. S6).

We also extend our theoretical calculations to determine the condensate velocity in response to an arbitrary force field f (supplementary material, Sec. SIII C). In the case where this force incorporates both attractive and repulsive RNA–protein interactions ($\gamma > 0$), we find that as the condensate-promoter distance decreases, the velocity peaks at a distance greater than the condensate radius and then drops to zero, meaning the droplet stops

short of colocalizing with the promoter. Increasing the strength of protein–RNA repulsion γ decreases the peak condensate velocity and increases the distance at which the condensate halts its motion. If the droplet's initial position is below this distance from the promoter, our calculations predict it will flow away from the RNA source.

To characterize how the directed motion of the droplet in response to a force f compares to passive Brownian motion of the droplet with diffusion coefficient D_{eff} , we calculate a macroscopic Péclet number in d dimensions ([supplementary material](#), Sec. SIII D),

$$\text{Pe} = \frac{vR}{D_{\text{eff}}} = \frac{V_D \Delta c}{2d^2} \left| \int_D \frac{d^d z}{V_D} \frac{Rf}{k_B T} \right|, \quad (10)$$

where R is the condensate radius. Note that the macroscopic Péclet number scales with the number of molecules inside the droplet and the microscopic Péclet number, $Rf/k_B T$, averaged over the droplet volume V_D . Hence, one can easily reach high Péclet numbers if condensates contain sufficiently many proteins.

IV. DIRECTED MOTION OF ENHANCER-BOUND CONDENSATES CAN INCREASE ENHANCER-PROMOTER CONTACTS

Overall, our theory and simulations show that RNA concentration gradients can lead to the long-range attraction of protein droplets toward an actively transcribing gene promoter. We next asked whether the directed motion of condensates, in collaboration with loop extrusion by cohesin, would influence the proximity of the enhancer and the promoter. We consider the dynamics of the intervening chromatin polymer, which we model as a Rouse chain.⁶⁴ Despite neglecting many details of chromatin structure, Rouse models have generated many insights into polymer dynamics and have been shown to recapitulate dynamical data on chromosomes.^{59,65,66}

The 3D distances between two loci connected by a Rouse chain of length L_C follow a Maxwell distribution $P(r) = 4\pi r^2 (3/(4L_c \ell_p))^3/2 \exp(-3r^2/(4L_c \ell_p))$ where ℓ_p is the persistence length of chromatin. If there are non-overlapping, non-interacting loops in between the two loci, the intervening distance distribution has a reduced effective contour length L_C .⁶⁷ Live-cell imaging experiments estimate that loop extrusion with boundaries reduces the effective genomic separation between two CTCF loci by 61%.⁵⁹ Therefore, rather than simulating the actual loop extrusion process, which requires introducing several parameters such as the extrusion speed and residence time of cohesin on DNA,⁶⁸ in this work, we simply assume a reduced contour length to model the effect of cohesin on enhancer–promoter distances.

Active transcription at a gene promoter results in an RNA concentration gradient, which attracts an enhancer-bound condensate toward the promoter, but not vice versa. In the absence of measurements detailing how enhancer DNA is organized within the condensate, we coarse-grain the enhancer locus as a single monomer within a Rouse chain. Assuming the condensate is strongly tethered to the enhancer locus, we assume additivity of forces so that the enhancer velocity is simply a sum of the directed velocity of a

free condensate in an RNA gradient and the Rouse dynamics in the absence of a condensate.

In 3D, the velocity of a free spherical condensate of radius R at a distance r away from a point source of RNA has a closed analytical expression ([supplementary material](#), Sec. SIII)

$$v(r) = v\tilde{v} = \frac{v}{r^2} \left[e^{-\frac{R+r}{\ell}} (\ell + R) (\ell + r) - e^{-\frac{|R-r|}{\ell}} (\ell^2 - Rr + \ell|R - r|) \right], \quad (11)$$

where $\ell = \sqrt{M_m/k_d}$ is the diffusion length of RNA and v sets the velocity scale

$$v = \frac{3M_c \chi k_p c_- \ell}{2\Delta c(4\pi R^3/3)D_m}, \quad (12)$$

such that \tilde{v} is dimensionless. As seen in [Fig. 2\(b\)](#), the dimensionless velocity is sharply peaked at the droplet radius $r = R$ and then decays according to the gradient of RNA. Therefore, the characteristic length scale over which the droplet can sense the promoter is given by the sum of the droplet radius and the diffusion length of RNA, ℓ . Here, we use a droplet radius of $R = 250$ nm based on measurements of transcriptional condensates *in vivo*^{32,35} and estimate the RNA diffusion length to be $\ell = 4.24 \mu\text{m}$ ([supplementary material](#), Sec. VI). The magnitude of the velocity, v , additionally depends on gene-specific parameters, such as the RNA production rate k_p . We thus treat v as a parameter that we vary in our Brownian dynamics simulations.

Incorporating a non-reciprocal force into the Rouse chain dynamics will lead to probability currents and a steady state that cannot be described by a Boltzmann weight. To calculate this non-equilibrium steady state distribution, we perform Brownian dynamics simulations of a discretized Rouse chain, where each monomer represents a Kuhn segment of length $b = 2\ell_p$. We choose a Kuhn length of 35.36 nm (441.42 bp) based on predictions from a “zig-zag” polymer model of nucleosome-bound DNA in mouse embryonic stem cells,⁶⁹ which is consistent with Ref. 70. The dynamics of the monomers $n \in [1, N]$ connected by Hookean springs k is given by

$$\partial_t \mathbf{r}_n(t) = \xi_n^{-1} k \Delta_n \mathbf{r}_n(t) + \boldsymbol{\eta}_n(t) + v\tilde{v}(r_{ep}) \hat{\mathbf{r}}_{ep} \delta_{ne}, \quad (13)$$

where Δ_n is the discrete Laplacian. The enhancer locus, indicated by monomer index e , persistently moves in the direction of the promoter, $\hat{\mathbf{r}}_{ep}$, with a velocity that depends on the distance r_{ep} between the enhancer and the promoter [cf. Eq. (11)]. The random excitations $\boldsymbol{\eta}_n(t)$ have zero mean and in general have a covariance that depends on the friction ξ_n and activity A_n of each locus.⁷¹

$$\langle \boldsymbol{\eta}_n(t) \cdot \boldsymbol{\eta}_m(t') \rangle = \sqrt{A_n A_m / \xi_n \xi_m} \delta(t - t') \delta_{nm}. \quad (14)$$

We assume that all monomers except for the enhancer (and potentially the promoter) have identical activity and friction with average diffusion coefficient $D_c = A_0/\xi_0$. However, we expect that the presence of a large condensate with a radius $R = 250$ nm at the enhancer would increase the Stokes friction ξ_e by a factor of $2R/b \approx 14$. Different choices for the friction and activity of the enhancer do not qualitatively change our results ([supplementary material](#), Fig. S13). In our simulations, we set $b = 1$ and $D_c = 1$ for simplicity but convert to experimental length and time scales using the Kuhn length $b = 35.6$ nm and the apparent diffusivity of chromatin $D_{\text{app}} = 0.01 \mu\text{m}^2/\text{s}^{1/2}$ ([supplementary material](#), Sec. VI).

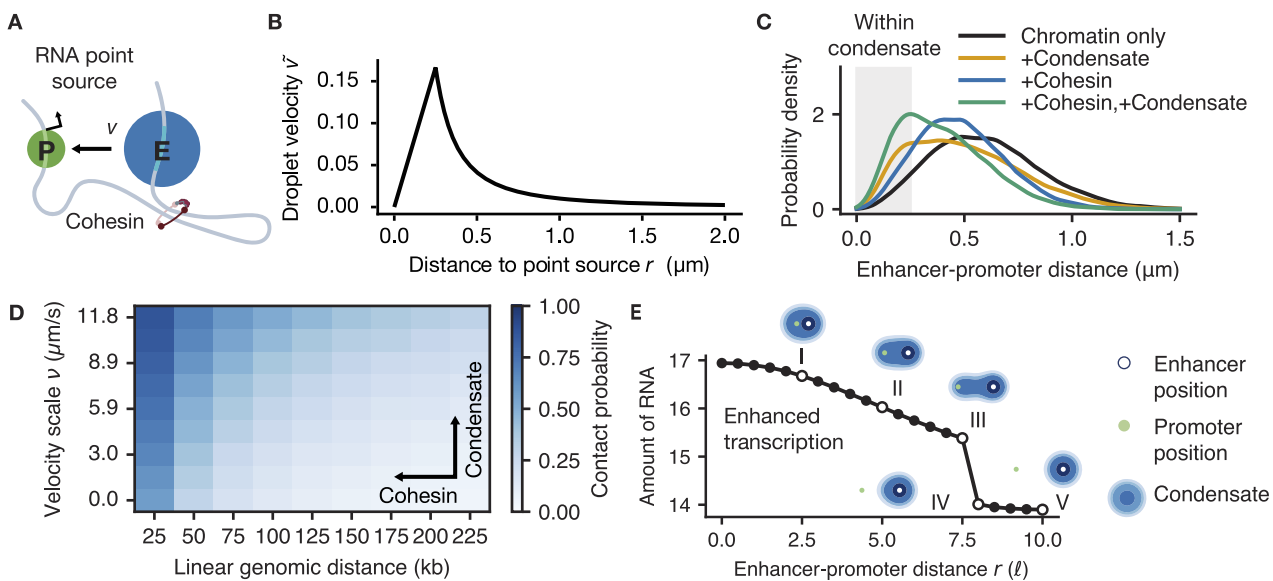


FIG. 2. Directed motion of enhancer-bound condensates can contribute to enhancer–promoter proximity, and hence, enhanced transcription at the promoter. (a) We calculate the distribution of enhancer–promoter separations using a polymer model that takes into account loop extrusion by cohesin and the directed motion of an enhancer-bound condensate toward the promoter. (b) Dimensionless droplet velocity in response to an RNA point source in 3D [Eq. (11)], which resembles an effective attractive force moving the enhancer toward the promoter [Eq. (13)]. Here, we use a droplet radius of $R = 250 \text{ nm}$ based on measurements of transcriptional condensates *in vivo*^{32,35} and estimate the RNA diffusion length to be $\ell = 4.24 \mu\text{m}$ (supplementary material, Sec. SVI). (c) Distribution of separations between an enhancer and promoter that are 150 kbp apart. The presence of an enhancer-bound condensate and transcription at the promoter shifts the distribution to smaller separations (in this example, the velocity prefactor is $v = 10 \mu\text{m s}^{-1}$). Cohesin also brings enhancers closer to promoters by reducing the effective contour length of the intervening polymer (in this example, by a factor of 2/3). Both of these effects collaborate to bring the enhancer within a condensate radius of the promoter. (d) The enhancer–promoter contact probability as a function of the contour length of chromatin connecting the two loci and the magnitude of the condensate velocity toward the promoter. We define the contact probability as the probability that the enhancer–promoter distance is within the radius of the condensate, assumed to be 250 nm. (e) For a fixed enhancer–promoter separation, our simulations show that RNA transcription is enhanced at the promoter when the condensate overlaps with the gene promoter.

In the following, we assume that the RNA concentration gradient and the enhancer-bound condensate are stable on the timescales for the polymer dynamics to reach steady state. This assumption is reasonable, since the lifetime of the RNA gradient depends on the lifetime of nascent RNA, which is around 10 minutes.⁷² Condensates localized to super-enhancers have been reported to remain stable for a similar timescale,³² which is much larger than the estimated Rouse time for a 100 kbp chain—on the order of 10 seconds (supplementary material, Sec. SVI). Nonetheless, condensate-promoter contact could alter transcription rates at the promoter, thereby either strengthening condensate-promoter interactions via positive feedback or potentially dissolving or repelling the condensate via negative feedback. This would be a very interesting extension of the model and is reserved for future studies. For the purposes of this work, we neglect such feedback loops and calculate the steady-state enhancer–promoter distance distribution from an ensemble of 2000 snapshots across 200 independent simulations.

Cohesin-mediated loop extrusion effectively reduces the enhancer–promoter (E–P) tether length, resulting in a decreased mean enhancer–promoter distance [Fig. 2(c), blue line]. The velocity of the condensate is largest in a finite range near the condensate’s radius [Fig. 2(b)]. Hence, the directed motion of the condensate shifts the probability density from large enhancer–promoter

distances to distances that are within the condensate’s radius [Fig. 2(c), yellow line]. Our simulations show that cohesin and the condensate can collaboratively increase the probability of enhancer–promoter contacts [Fig. 2(c), green line]. We find that the contact probability decreases with increasing linear genomic distance, which conversely implies that it increases in the presence of cohesin [Fig. 2(d)]. In addition, the contact probability increases with the condensate velocity v [Fig. 2(d)], which is proportional to the transcription rate at the promoter k_p [Eq. (12)]. Due to the finite range in which the condensate velocity is maximized, the contact probability is less sensitive to changes in the condensate velocity v for larger genomic distances (supplementary material, Fig. S12). In contrast, cohesin would on average compact any genomic enhancer–promoter distance by the same factor, which we assume to be 2/3 based on live-cell imaging studies.⁵⁹ Therefore, we propose that cohesin can first reel long-distance enhancers toward promoters, followed by an additional condensate-mediated increase in enhancer–promoter contacts.

We next wondered how an increased contact probability affects transcription at the promoter locus. To investigate this question, we return to our phase field simulations where the transcription rate is proportional to the protein concentration. The condensate may be “tethered” to the enhancer locus because of protein-mediated interactions. To model this approximately, we introduce a term to Eq. (3)

that represents an attractive Gaussian potential toward the enhancer at a fixed position \mathbf{r}_e

$$\mathcal{F}_{ce}(c, \mathbf{r}_e) = \int d^d r \left[\eta \exp\left(-\frac{|\mathbf{r} - \mathbf{r}_e|^2}{2\sigma_e^2}\right) c \right], \quad (15)$$

and initialize the droplet at the enhancer. Note that the use of a potential in the free energy is an approximation for a possibly non-equilibrium driving force that “tethers” the condensate.

We find that the amount of RNA produced at the promoter increases sharply below a fixed enhancer–promoter distance [Fig. 2(e)]. This long-range effect of an enhancer on transcription has been described in the literature as the “action-at-a-distance” model.⁴⁵ In our model, transcription at the promoter is enhanced once the enhancer-bound condensate touches the promoter. For a perfectly round droplet, this is the case when the enhancer–promoter distance matches the radius of the condensate. In our simulations, the droplet elongates when the attraction of proteins toward RNA at the promoter-proximal interface outcompetes the attraction of the droplet to the enhancer and surface tension. Droplet elongation allows the condensate to stretch toward the promoter and enhance transcription at larger enhancer–promoter distances than if the droplet remained circular [snapshots II and III, Fig. 2(e)].

According to the “action-at-a-distance” model, we expect the effective transcription rate to be linear in the contact probability, which increases with cohesin and the condensate. However, past experimental studies have shown how transcription can have a nonlinear dependence on enhancer–promoter contact probability.⁴⁴ In other words, once a threshold in contact probability is exceeded, further increases in contact probability do not have a significant effect on transcription. For a fixed condensate velocity v , enhancer–promoter pairs at small genomic separations already have a contact probability that exceeds this threshold, independent of cohesin-mediated compaction [Fig. 2(d)]. However, for distal enhancer–promoter pairs, the condensate velocity v is insufficient to bring the enhancer–promoter contact probability above the threshold. In these cases, cohesin is required to first bring the enhancer within a range where gradient-sensing by the condensate can bridge the remaining gap. These findings could explain recent experimental results that suggest transcription is dependent on cohesin for genetically distant enhancer–promoter pairs but independent for genetically proximal pairs.^{50,51}

V. CONDENSATES CAN EXHIBIT OSCILLATIONS IN MORPHOLOGY AND DISTANCE TO THE PROMOTER

Live-cell imaging experiments have observed condensates moving toward and away from promoters, resulting in dynamic “kissing” interactions.^{32,35} In the cell, the transcription machinery enriched within transcriptional condensates first assembles into the preinitiation complex. RNA polymerase II then stalls near the promoter during promoter-proximal pausing before finally proceeding to the productive elongation of RNA.^{60–62} These processes give rise to an effective time delay between condensate-promoter contact and transcription. Hence, we next investigate whether such a delay could lead to oscillations in the condensate position relative to the promoter. We modify the reaction–diffusion model to incorporate a time delay

τ into the transcription rate and also to increase the sensitivity of the transcription rate to changes in the protein concentration,

$$\partial_t m = \nabla \cdot (M_m \nabla m) + k_p(\mathbf{r}_p | \sigma_p) f_+(c(t - \tau)) - k_d m, \quad (16)$$

where $k_p(\mathbf{r}_p | \sigma_p)$ is the Gaussian production rate that we previously used in Eq. (5). We introduce a Hill function $f_+(c)$ to increase the sensitivity of the transcription rate to changes in the protein concentration (supplementary material, Sec. SIX). In this model, proteins respond immediately to the concentration profile of RNA, whereas the RNA profile adjusts according to the protein distribution from a previous time. We hypothesize that a delayed response of transcription to condensate-promoter contact, in combination with negative feedback between the protein and RNA, could lead to oscillations. In particular, accumulation of RNA at the promoter leads to charge repulsion, which could expel the condensate from the promoter.

To test these ideas, we now also consider the reentrant repulsion term, $\gamma c^2 m^2$, in the RNA–protein interaction energy [Eq. (2)] and simulate circular protein droplets using the same initial conditions as in Sec. III. When the condensate is far from the promoter, RNA concentrations are low and the attraction term χcm dominates [Eq. (2)], causing the condensate to move towards the promoter. When the condensate overlaps with the promoter, it enhances transcription after the time delay τ . As a result, the RNA concentration increases roughly 3.5-fold due to the increased sensitivity of the transcription rate to changes in protein concentration [Fig. 3(a)]. At high RNA levels, the repulsion term $\gamma c^2 m^2$ dominates [Eq. (2)], expelling protein away from the promoter and returning the system to its basal rate of transcription [Fig. 3(a)].

The droplet exhibits two distinct types of oscillations. It can either cycle through various bean-shaped morphologies [Fig. 3(b)] or alternate between a vacuole and a whole droplet [Fig. 3(c)]. The type of oscillation that occurs depends on whether the repulsion strength and delay allow the droplet to fully colocalize with the promoter before RNA production is enhanced by condensate-promoter overlap. When the droplet colocalizes with the promoter, the increased RNA levels push the droplet away symmetrically, forming a vacuole. When the droplet does not fully colocalize with the promoter, the increased RNA levels push it asymmetrically, forming a bean-shaped morphology. With strong repulsions $\gamma \geq 0.035$, the droplet can never fully colocalize with the promoter even with an infinite time delay. Hence, the system oscillates between bean-like morphologies with different extents of condensate-promoter overlap [Fig. 3(b)]. For weaker repulsions ($\gamma = 0.02, 0.025, 0.03$), the droplet can fully colocalize with the promoter given enough time, leading to symmetric oscillations centered at the origin, where a vacuole forms and refills [Fig. 3(c)]. Reducing the time delay for these weaker repulsions leads to bean-like morphologies, because there is not enough time for the droplet to flow and fully colocalize with the promoter at the origin.

The system oscillates only above a critical repulsion strength and time delay [Fig. 3(d), gray line]. The critical time delay is determined by the timescale for the condensate to flow toward the promoter from its initial position. This timescale increases as a function of the repulsion strength γ , since repulsion slows down condensate motion, as shown in our theoretical calculations (supplementary material, Sec. SIII C). There is also a critical repulsion strength below which oscillations do not occur. In this regime,

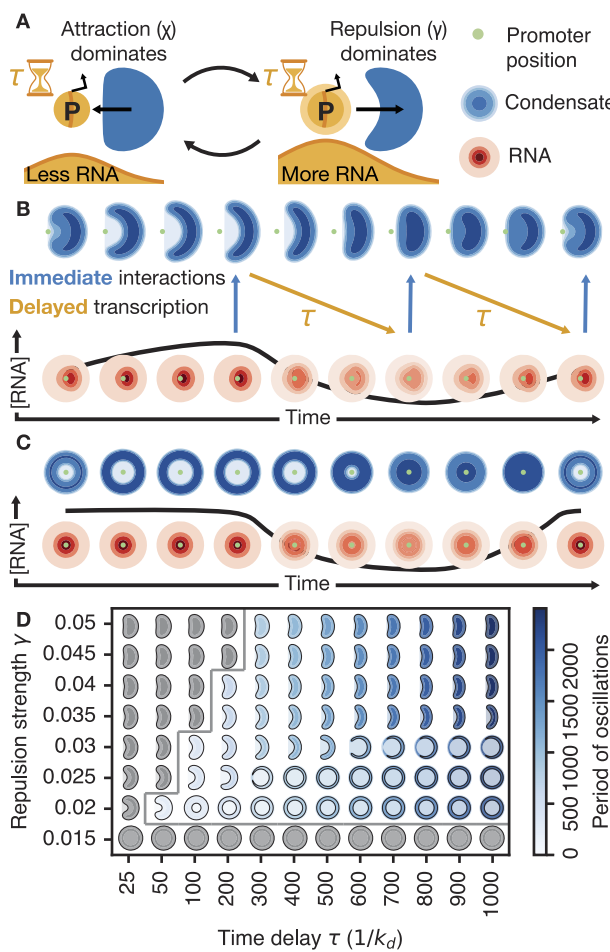


FIG. 3. Condensate morphologies and RNA concentrations show oscillations when protein–RNA repulsion is sufficiently strong and transcription responds to the protein droplet after a delay time τ . (a) We consider a system where transcription at the promoter responds to the presence of transcriptional proteins after a fixed time delay. When the condensate overlaps with the promoter, increased transcription leads to an accumulation of RNA at the promoter. The resulting charge repulsion pushes the droplet away and deforms its shape. (b) Simulated trajectory of bean-like droplets (blue) and the RNA concentration field (red) over time with $\gamma = 0.03$ and $\tau = 250$. The condensate morphology immediately responds to the concurrent RNA field, while transcription responds to a morphology from a previous time. (c) With $\gamma = 0.02$ and $\tau = 250$, condensate morphologies oscillate between vacuoles and circular droplets (blue) in response to oscillating, radially symmetric RNA concentration fields (red). (d) Oscillations occur above a critical time delay and repulsion strength (indicated by the gray lines). The period of oscillations (color bar) increases with the time delay. The repulsion strength determines the extent to which droplets colocalize with the promoter, which in turn determines the droplet morphology. Simulation parameters: $\alpha = 1$, $\beta = -0.25$, $\kappa = 0.05$, $\chi = -0.1$, $M_c = 1$, $D_m = 1$, $k_p = 0.2$, $\sigma_p = 2.5$, and $k_d = 1$.

the dynamics are dominated by the attractive protein–RNA interactions, even with transcription enhanced by the droplet, causing the droplet to reach a steady state where it simply colocalizes with the promoter. In summary, for fixed time delay, we predict that there is a “Goldilocks zone” of repulsion strengths that permit condensate-promoter oscillations [Fig. 3(d)].

The period of oscillations increases as $\sim 2\tau$ [Fig. 3(d), color bar] and corresponds to 2τ plus an additional traversal time (supplementary material, Figs. S19 and S20). This is because the droplet spends a time τ in the promoter-proximal and the promoter-distal positions and requires some additional amount of time to traverse between these locations [Figs. 3(b) and 3(c)]. The period of oscillations is insensitive to the repulsion strength (supplementary material, Fig. S19). Overall, these results demonstrate that RNA concentrations and condensate morphologies can oscillate when transcription is delayed with respect to condensate-promoter contact. However, these results show oscillations in condensate morphology, which are different from the oscillations in condensate-promoter distance or dynamic “kissing,” observed in live-cell imaging experiments.^{32,35}

Therefore, we finally explore the conditions necessary for our system to exhibit center-of-mass oscillations. The droplet has no momentum under the overdamped dynamics of our system. Consequently, the center-of-mass displacement is solely determined by the range of RNA-mediated condensate attraction and repulsion, which can be extended by increasing the RNA diffusion length. We accomplish this by decreasing the degradation rate while maintaining the same concentration at the origin [Figs. 4(a) and 4(b)]. When the diffusion length is larger than the size of the condensate, we find that the droplet can show center-of-mass oscillations [Fig. 4(c)]. The distance oscillations are in phase with oscillations

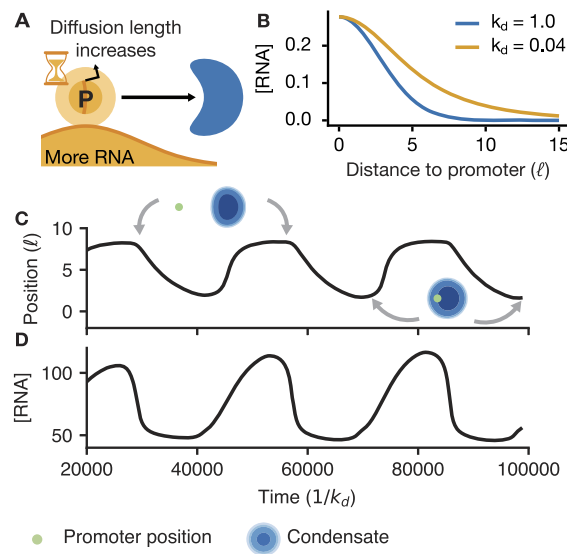


FIG. 4. Condensates can show center-of-mass oscillations when the RNA diffusion length is larger than the condensate’s size. (a) Increasing the RNA diffusion length leads to a larger displacement of the droplet in response to RNA repulsion. (b) Decreasing the RNA degradation rate k_d increases the diffusion length. We adjust the production rate such that the peak RNA concentration is unchanged. (c) Simulated trajectory shows the condensate moving towards and away from the promoter. The promoter (marked in green) is centered at the origin. (d) The RNA concentration is in phase with the condensate-promoter separation. Simulation parameters: $\alpha = 1$, $\beta = -0.25$, $\kappa = 0.05$, $\chi = -0.1$, $\gamma = 0.06$, $M_c = 1$, $D_m = 1$, $k_p = 0.0138$, $\sigma_p = 2.5$, $k_d = 0.04$, and $\tau = 12\,000$.

in the RNA concentration due to the delayed response of transcription to condensate-promoter contact [Fig. 4(d)]. Our simulations are thus most consistent with a “hit and run” or “kiss and kick” picture of enhancer–promoter communication, where transcription is enhanced after the condensate has already moved away from the promoter.^{56,73} Together, these results show that the combined effects of RNA-mediated directed motion, RNA-driven reentrant phase transitions, and time delays in gene bursting provide one possible explanation for the dynamic co-localization of transcriptional condensates with gene promoters.

VI. DISCUSSION

We have explored how protein condensates respond to an RNA transcription site (source) due to electrostatic interactions between proteins and RNA. Depending on the protein concentration and the RNA production rate, we found that the condensate can either move gradually toward the RNA source or dissolve and renucleate at the transcription site. Analytical calculations, in agreement with simulations, show that in the case of droplet motion, the droplet velocity is a non-monotonic function of the distance to the transcription site and peaks at a distance corresponding to the condensate radius. Interestingly, our calculations show that the liquid droplet, in d dimensions, moves d times faster than the individual proteins that make up the condensate. This enhancement in velocity is due to a $d - 1$ -dimensional flux of material through the light phase that continuously nucleates the leading edge of the droplet as it moves.²⁶ In addition, material in the dense phase moves in the direction of the RNA gradient from the trailing edge to the leading edge.^{26,27} Gene-specific parameters such as the transcription rate determine the steepness of the RNA concentration gradient, which in turn influences the speed of the droplet that senses this gradient.

In the present paper, condensate motion is driven by interactions with RNA in the bulk of the droplets and does not require hydrodynamic couplings *per se*. This mechanism stands in contrast with droplet propulsion due to the Marangoni effect²⁵ and to the diffusiophoresis of colloids, where solute interactions with the colloidal surface lead to tension gradients and a slip velocity against the solvent.⁷⁴ Although directed motion of transcriptional condensates has yet to be observed in experiments, the mechanism we identify is general for any droplet in a concentration gradient. For example, *in vitro*, it has been observed that salt concentration gradients induce phoretic condensate motion.⁴¹ We speculate that this mechanism could also contribute to the observed motion of nuclear speckles and Cajal bodies *in vivo*.^{36–38,75}

We next explored the consequences of directed motion of protein condensates toward actively transcribing promoters for enhancer–promoter communication. Since a transcriptional condensate is assumed to be bound to the enhancer locus,³² its motion leads to a non-reciprocal attractive interaction between the enhancer and the promoter. Brownian dynamics simulations of the intervening chromatin chain show that directed motion increases the contact probability between the condensate and the promoter. This effect is more pronounced for genetically close enhancer–promoter pairs, since the condensate velocity is distance-dependent. In contrast, loop extrusion by cohesin should linearly compact the enhancer–promoter distance for any genomic separation between the enhancer and the promoter. We hypothesize that cohesin could

reel in long-range enhancers, while directed motion of condensates could act at short and intermediate scales. Together, cohesin and condensates thus mediate a multi-scale enhancer–promoter attraction.

For genetically close enhancer–promoter pairs, condensate directed motion could provide a compensatory mechanism that allows for enhancer–promoter “microcompartments” (contacts) that are robust to cohesin depletion.^{48,53,54} The increase in enhancer–promoter contact probability due to condensates alone could also explain why transcription appears to be cohesin-independent for genes with genetically close enhancers but cohesin-dependent for genes with distal enhancers.^{50,51} Consistent with our proposed mechanism, depletion of the Mediator complex, which is a key component of transcriptional condensates, decreases enhancer–promoter interactions and associated gene expression levels.⁷⁶ However, future experiments could more directly test whether disrupting condensate stability or motion has an influence on enhancer–promoter contacts.⁷⁷ Future theoretical studies of multi-component condensates could also predict how specific molecular components affect condensate motion.

Future work could explore cohesin and condensate based mechanisms of gene regulation in more dynamic detail. For instance, the assumption that cohesin simply compacts the tether length connecting the enhancer and promoter fails to take into account the active dynamics of loop extrusion. Other literature has suggested that loop extrusion could drag a promoter toward the surface of the condensate, leading to a nonmonotonic dependence of the enhancer–promoter contact probability on genomic distance.⁷⁸ In addition, in this work, we focus on steady state contact probabilities; however, the emergence of time-resolved live cell imaging data could enable direct visualization of the enhancer–promoter first-passage process.^{79–81} Comparisons to such data would require simulating the active dynamics of loop extrusion, accounting for the finite lifetime of condensates and RNA gradients,³² and calculating the first passage time to contact. Our polymer model could also be extended to couple the transcription rate at the promoter to the enhancer–promoter contact probability. Increased transcription would initially increase the velocity of enhancer-bound condensates and, therefore, the enhancer–promoter contact probability, leading to positive feedback.^{44,82} Eventually, accumulation of RNA could lead to charge repulsion, which dissolves or expels the condensate, regulating the contact process in a complex way.

In this work, for simplicity, we have neglected the molecular interactions of individual proteins with chromatin^{5,83} and instead modeled the condensate as a single, large monomer of the chromatin polymer. Future work could incorporate the co-condensation of DNA with the proteins within the condensate, which increases the tension on the DNA chain.⁸⁴ Condensates have also been shown to mechanically exclude chromatin and pull together chromatin loci.^{85,86} Other theoretical works have proposed that the polymer chain connecting the enhancer and promoter may be confined to the surface of the condensate.⁸⁷ There remains much to learn about how condensates interact with DNA, indicating that further work is needed to determine the most appropriate approach for the multi-scale modeling of condensate-chromatin systems.⁸⁸

Finally, we have shown that transcriptional condensates can show oscillations in morphology and in the distance to the promoter. Bean-shaped condensates and vacuoles have previously been

reported as nonequilibrium steady states²⁹ and observed in experiment.⁴⁰ We demonstrate that dynamic cycling between these states requires a time delay between condensate-promoter contact and negative feedback due to RNA accumulation at the promoter.¹² Such a delay is plausible biologically, due to the multiple internal state changes that the promoter undergoes prior to productive elongation of RNA. Oscillatory dynamics are possible as long as the time delay from promoter-proximal pausing is greater than the timescale for the droplet to flow toward the promoter. While directed motion of transcriptional condensates has yet to be measured, nuclear speckles show directed motion with velocities between 0.2 and 1.5 $\mu\text{m s}^{-1}$. The resulting timescale to traverse a typical enhancer–promoter separation of $\sim 1 \mu\text{m}$ is ~ 1 min, which is indeed less than the lifetime of RNA polymerase II in a paused state.

Unlike the condensate-promoter kissing events observed in Refs. 32 and 35, our model predicts that the RNA levels at the promoter are in phase with the condensate-promoter distance (out of phase with condensate-promoter contact). That is, transcription is enhanced after the condensate has moved away from the promoter, due to the time delay. Therefore, our model could provide a mechanistic basis for the proposed “hit and run” or “kiss and kick” model of enhancer–promoter communication.^{56,73} More generally, our work demonstrates that phase separation of transcriptional proteins coupled with RNA production and degradation can yield rich dynamics with potentially far-reaching consequences for gene regulation.

SUPPLEMENTARY MATERIAL

The [supplementary material](#) provides derivations, unit conversions, additional details on simulations and analysis, and additional figures.

ACKNOWLEDGMENTS

The authors acknowledge Mehran Kardar and Yannick Azhri Din Omar for their insightful discussions. We also acknowledge Mehran Kardar for the critical reading of the paper. We acknowledge Thomas Nok Hin Cheng and the MIT Chemical Engineering Communication Lab for their feedback on figure presentation. This work was supported by the National Science Foundation, through the Biophysics of Nuclear Condensates (Grant No. MCB-2044895). A.G. was also supported by an EMBO Postdoctoral Fellowship (Grant No. ALTF 259-2022). D.K. was supported by a National Science Foundation Graduate Research Fellowship under Grant No. 2141064 and an internal MIT Fellowship. A.K.C. and D.G. were also supported by the Ragon Institute. The authors acknowledge the MIT SuperCloud and Lincoln Laboratory Supercomputing Center for providing HPC resources that have contributed to the research results reported within this paper.

AUTHOR DECLARATIONS

Conflict of Interest

A.K.C. is a consultant for Flagship Pioneering and its affiliated companies, Apriori Bio and Metaphore Bio. He holds equity in these companies and in Dewpoint Therapeutics.

Author Contributions

D.G., D.K., and P.N. contributed equally to this work.

David Goh: Conceptualization (equal); Data curation (lead); Formal analysis (equal); Investigation (equal); Methodology (equal); Software (lead); Visualization (lead); Writing – original draft (equal); Writing – review & editing (equal). **Deepti Kannan:** Conceptualization (equal); Formal analysis (equal); Investigation (equal); Methodology (equal); Software (equal); Visualization (equal); Writing – original draft (equal); Writing – review & editing (equal). **Pradeep Natarajan:** Conceptualization (equal); Methodology (equal); Software (equal); Visualization (equal); Writing – original draft (supporting); Writing – review & editing (supporting).

Andriy Goychuk: Conceptualization (equal); Formal analysis (equal); Investigation (equal); Methodology (equal); Software (equal); Writing – original draft (equal); Writing – review & editing (equal). **Arup K. Chakraborty:** Conceptualization (equal); Funding acquisition (lead); Investigation (equal); Project administration (lead); Resources (lead); Supervision (lead); Writing – original draft (equal); Writing – review & editing (equal).

DATA AVAILABILITY

All simulation and analysis scripts are available on GitHub in the following repositories: 1. Finite volume simulations (FVM) are at <https://github.com/gohdavid/CoupledEPCondensates>. 2. Brownian Dynamics (BD) simulations are at <https://github.com/gohdavid/active-polymers>. 3. Theoretical calculations (Theory) are at <https://github.com/gohdavid/CoupledEPCondensatesTheory>. 4. Finite Element Simulations (FEM) are at <https://github.com/gohdavid/CoupledEPCondensatesFEM>. The notebooks used to generate the figures in this work are in each of these repositories. Although we do not include simulation data due to storage limitations, we include the simulation scripts used to generate the data. All simulation and analysis scripts have also been deposited in Zenodo (<https://doi.org/10.5281/zenodo.17049160>).

REFERENCES

- 1 S. F. Banani, H. O. Lee, A. A. Hyman, and M. K. Rosen, “Biomolecular condensates: Organizers of cellular biochemistry,” *Nat. Rev. Mol. Cell Biol.* **18**, 285–298 (2017).
- 2 Y. Shin and C. P. Brangwynne, “Liquid phase condensation in cell physiology and disease,” *Science* **357**, eaaf4382 (2017).
- 3 A. A. Hyman, C. A. Weber, and F. Jülicher, “Liquid-liquid phase separation in Biology,” *Annu. Rev. Cell Dev. Biol.* **30**, 39–58 (2014).
- 4 P. Li, S. Banjade, H.-C. Cheng, S. Kim, B. Chen, L. Guo, M. Llaguno, J. V. Hollingsworth, D. S. King, S. F. Banani, P. S. Russo, Q.-X. Jiang, B. T. Nixon, and M. K. Rosen, “Phase transitions in the assembly of multivalent signalling proteins,” *Nature* **483**, 336–340 (2012).
- 5 K. Shrinivas, B. R. Sabari, E. L. Coffey, I. A. Klein, A. Boija, A. V. Zamudio, J. Schuijers, N. M. Hannett, P. A. Sharp, R. A. Young, and A. K. Chakraborty, “Enhancer features that drive formation of transcriptional condensates,” *Mol. Cell* **75**, 549–561.e7 (2019).
- 6 J. A. Morin, S. Wittmann, S. Choubey, A. Klosin, S. Golfier, A. A. Hyman, F. Jülicher, and S. W. Grill, “Sequence-dependent surface condensation of a pioneer transcription factor on DNA,” *Nat. Phys.* **18**, 271–276 (2022).
- 7 J. Berry, S. C. Weber, N. Vaidya, M. Haataja, and C. P. Brangwynne, “RNA transcription modulates phase transition-driven nuclear body assembly,” *Proc. Natl. Acad. Sci. U. S. A.* **112**, E5237–E5245 (2015).

- ⁸H. Zhang, S. Elbaum-Garfinkle, E. M. Langdon, N. Taylor, P. Occhipinti, A. Bridges, C. Brangwynne, and A. Gladfelter, "RNA controls PolyQ protein phase transitions," *Mol. Cell* **60**, 220–230 (2015).
- ⁹M. Feric, N. Vaidya, T. S. Harmon, D. M. Mitrea, L. Zhu, T. M. Richardson, R. W. Kriwacki, R. V. Pappu, and C. P. Brangwynne, "Coexisting liquid phases underlie nucleolar subcompartments," *Cell* **165**, 1686–1697 (2016).
- ¹⁰P. R. Banerjee, A. N. Milin, M. M. Moosa, P. L. Onuchic, and A. A. Deniz, "Reentrant phase transition drives dynamic substructure formation in ribonucleoprotein droplets," *Angew. Chem., Int. Ed.* **56**, 11354–11359 (2017).
- ¹¹A. N. Milin and A. A. Deniz, "Reentrant phase transitions and non-equilibrium dynamics in membraneless organelles," *Biochemistry* **57**, 2470–2477 (2018).
- ¹²J. E. Henninger, O. Oksuz, K. Shrinivas, I. Sagi, G. LeRoy, M. M. Zheng, J. O. Andrews, A. V. Zamudio, C. Lazaris, N. M. Hannett, T. I. Lee, P. A. Sharp, I. I. Cisse, A. K. Chakraborty, and R. A. Young, "RNA-mediated feedback control of transcriptional condensates," *Cell* **184**, 207–225.e24 (2021).
- ¹³C. A. Weber, D. Zwicker, F. Jülicher, and C. F. Lee, "Physics of active emulsions," *Rep. Prog. Phys.* **82**, 064601 (2019); [arXiv:1806.09552](https://arxiv.org/abs/1806.09552).
- ¹⁴S. C. Glotzer, E. A. Di Marzio, and M. Muthukumar, "Reaction-controlled morphology of phase-separating mixtures," *Phys. Rev. Lett.* **74**, 2034–2037 (1995).
- ¹⁵D. Carati and R. Lefever, "Chemical freezing of phase separation in immiscible binary mixtures," *Phys. Rev. E* **56**, 3127–3136 (1997).
- ¹⁶J. D. Wurtz and C. F. Lee, "Chemical-reaction-controlled phase separated drops: Formation, size selection, and coarsening," *Phys. Rev. Lett.* **120**, 078102 (2018); [arXiv:1707.08433](https://arxiv.org/abs/1707.08433).
- ¹⁷J. Kirschbaum and D. Zwicker, "Controlling biomolecular condensates via chemical reactions," *J. R. Soc. Interface* **18**, 20210255 (2021); [arXiv:2103.02921](https://arxiv.org/abs/2103.02921).
- ¹⁸Y. I. Li and M. E. Cates, "Non-equilibrium phase separation with reactions: A canonical model and its behaviour," *J. Stat. Mech.: Theory Exp.* **2020**, 053206; [arXiv:2001.02563](https://arxiv.org/abs/2001.02563).
- ¹⁹D. Zwicker, A. A. Hyman, and F. Jülicher, "Suppression of Ostwald ripening in active emulsions," *Phys. Rev. E* **92**, 012317 (2015).
- ²⁰L. Demarchi, A. Goychuk, I. Maryshev, and E. Frey, "Enzyme-enriched condensates show self-propulsion, positioning, and coexistence," *Phys. Rev. Lett.* **130**, 128401 (2023); [arXiv:2301.00392](https://arxiv.org/abs/2301.00392).
- ²¹S. F. Banani, A. Goychuk, P. Natarajan, M. M. Zheng, G. Dall'Agnese, J. E. Henniger, M. Kardar, R. A. Young, and A. K. Chakraborty, "Active RNA synthesis patterns nuclear condensates," [bioRxiv 2024.10.12.614958](https://bioRxiv.org/abs/2024.10.12.614958) (2024).
- ²²R. Berthin, J. D. Fries, M. Jardat, V. Dahirel, and P. Illien, "Microscopic and stochastic simulations of chemically active droplets," *Phys. Rev. E* **111**, L023403 (2025).
- ²³D. Zwicker, R. Seyboldt, C. A. Weber, A. A. Hyman, and F. Jülicher, "Growth and division of active droplets provides a model for protocells," *Nat. Phys.* **13**, 408–413 (2017); [arXiv:1603.01571](https://arxiv.org/abs/1603.01571).
- ²⁴J. Decayaux, V. Dahirel, M. Jardat, and P. Illien, "Spontaneous propulsion of an isotropic colloid in a phase-separating environment," *Phys. Rev. E* **104**, 034602 (2021); [arXiv:2103.13244](https://arxiv.org/abs/2103.13244).
- ²⁵S. Michelin, "Self-propulsion of chemically active droplets," *Annu. Rev. Fluid Mech.* **55**, 77–101 (2023).
- ²⁶A. Goychuk, L. Demarchi, I. Maryshev, and E. Frey, "Self-consistent sharp interface theory of active condensate dynamics," *Phys. Rev. Res.* **6**, 033082 (2024); [arXiv:2401.17111](https://arxiv.org/abs/2401.17111).
- ²⁷C. A. Weber, C. F. Lee, and F. Jülicher, "Droplet ripening in concentration gradients," *New J. Phys.* **19**, 053021 (2017); [arXiv:1703.06276](https://arxiv.org/abs/1703.06276).
- ²⁸P. C. Bressloff, "Two-dimensional droplet ripening in a concentration gradient," *J. Phys. A: Math. Theor.* **53**, 365002 (2020).
- ²⁹H. H. Schede, P. Natarajan, A. K. Chakraborty, and K. Shrinivas, "A model for organization and regulation of nuclear condensates by gene activity," *Nat. Commun.* **14**, 4152 (2023).
- ³⁰D. Hnisz, K. Shrinivas, R. A. Young, A. K. Chakraborty, and P. A. Sharp, "A phase separation model for transcriptional control," *Cell* **169**, 13–23 (2017).
- ³¹B. R. Sabari, A. Dall'Agnese, A. Boija, I. A. Klein, E. L. Coffey, K. Shrinivas, B. J. Abraham, N. M. Hannett, A. V. Zamudio, J. C. Manteiga, C. H. Li, Y. E. Guo, D. S. Day, J. Schuijers, E. Vasile, S. Malik, D. Hnisz, T. I. Lee, I. I. Cisse, R. G. Roeder, P. A. Sharp, A. K. Chakraborty, and R. A. Young, "Coactivator condensation at super-enhancers links phase separation and gene control," *Science* **361**, eaar3958 (2018).
- ³²W.-K. Cho, J.-H. Spille, M. Hecht, C. Lee, C. Li, V. Grube, and I. I. Cisse, "Mediator and RNA polymerase II clusters associate in transcription-dependent condensates," *Science* **361**, 412–415 (2018).
- ³³S. Chong, C. Dugast-Darzacq, Z. Liu, P. Dong, G. M. Dailey, C. Cattoglio, A. Heckert, S. Banala, L. Lavis, X. Darzacq, and R. Tjian, "Imaging dynamic and selective low-complexity domain interactions that control gene transcription," *Science* **361**, eaar2555 (2018).
- ³⁴A. Boija, I. A. Klein, B. R. Sabari, A. Dall'Agnese, E. L. Coffey, A. V. Zamudio, C. H. Li, K. Shrinivas, J. C. Manteiga, N. M. Hannett, B. J. Abraham, L. K. Afeyan, Y. E. Guo, J. K. Rimel, C. B. Fant, J. Schuijers, T. I. Lee, D. J. Taatjes, and R. A. Young, "Transcription factors activate genes through the phase-separation capacity of their activation domains," *Cell* **175**, 1842–1855.e16 (2018).
- ³⁵M. Du, S. H. Stitzinger, J.-H. Spille, W.-K. Cho, C. Lee, M. Hijaz, A. Quintana, and I. I. Cisse, "Direct observation of a condensate effect on super-enhancer controlled gene bursting," *Cell* **187**, 331–344.e17 (2024).
- ³⁶M. Platani, I. Goldberg, J. R. Swedlow, and A. I. Lamond, "In vivo analysis of cajal body movement, separation, and joining in live human cells," *J. Cell Biol.* **151**, 1561–1574 (2000).
- ³⁷M. Platani, I. Goldberg, A. I. Lamond, and J. R. Swedlow, "Cajal body dynamics and association with chromatin are ATP-dependent," *Nat. Cell Biol.* **4**, 502–508 (2002).
- ³⁸S. M. Görisch, M. Wachsmuth, C. Ittrich, C. P. Bacher, K. Rippe, and P. Licher, "Nuclear body movement is determined by chromatin accessibility and dynamics," *Proc. Natl. Acad. Sci. U. S. A.* **101**, 13221–13226 (2004).
- ³⁹J. Kim, K. Y. Han, N. Khanna, T. Ha, and A. S. Belmont, "Nuclear speckle fusion via long-range directional motion regulates speckle morphology after transcriptional inhibition," *J. Cell Sci.* **132**, jcs226563 (2019).
- ⁴⁰A. Pancholi, T. Klingberg, W. Zhang, R. Prizak, I. Mamontova, A. Noa, M. Sobucki, A. Y. Kobitski, G. U. Nienhaus, V. Zuburdaev, and L. Hilbert, "RNA polymerase II clusters form in line with surface condensation on regulatory chromatin," *Mol. Syst. Biol.* **17**, e10272 (2021).
- ⁴¹V. S. Doan, I. Alshareedah, A. Singh, P. R. Banerjee, and S. Shin, "Diffusiophoresis promotes phase separation and transport of biomolecular condensates," *Nat. Commun.* **15**, 7686 (2024).
- ⁴²E. Jambon-Puillet, A. Testa, C. Lorenz, R. W. Style, A. A. Rebane, and E. R. Dufresne, "Phase-separated droplets swim to their dissolution," *Nat. Commun.* **15**, 3919 (2024).
- ⁴³X. Wang, M. J. Cairns, and J. Yan, "Super-enhancers in transcriptional regulation and genome organization," *Nucleic Acids Res.* **47**, 11481–11496 (2019).
- ⁴⁴J. Zuin, G. Roth, Y. Zhan, J. Cramard, J. Redolfi, E. Piskadlo, P. Mach, M. Kryzhanovska, G. Tihanyi, H. Kohler, M. Eder, C. Leemans, B. van Steensel, P. Meister, S. Smallwood, and L. Giorgetti, "Nonlinear control of transcription through enhancer-promoter interactions," *Nature* **604**, 571–577 (2022).
- ⁴⁵J. H. Yang and A. S. Hansen, "Enhancer selectivity in space and time: From enhancer-promoter interactions to promoter activation," *Nat. Rev. Mol. Cell Biol.* **25**, 574–591 (2024).
- ⁴⁶L. El Khattabi, H. Zhao, J. Kalchschmidt, N. Young, S. Jung, P. Van Blerkom, P. Kieffer-Kwon, K.-R. Kieffer-Kwon, S. Park, X. Wang, J. Krebs, S. Tripathi, N. Sakabe, D. R. Sobreira, S.-C. Huang, S. S. P. Rao, N. Pruitt, D. Chauss, E. Sadler, A. Lopez, M. A. Nóbrega, E. L. Aiden, F. J. Asturias, and R. Casellas, "A pliable mediator acts as a functional rather than an architectural bridge between promoters and enhancers," *Cell* **178**, 1145–1158.e20 (2019).
- ⁴⁷S. Cuartero, F. D. Weiss, G. Dharmalingam, Y. Guo, E. Ing-Simmons, S. Masella, I. Robles-Rebollo, X. Xiao, Y.-F. Wang, I. Barozzi, D. Djeghloul, M. T. Amano, H. Niskanen, E. Petretto, R. D. Dowell, K. Tachibana, M. U. Kaikonen, K. A. Nasmyth, B. Lenhard, G. Natoli, A. G. Fisher, and M. Merkenschlager, "Control of inducible gene expression links cohesion to hematopoietic progenitor self-renewal and differentiation," *Nat. Immunol.* **19**, 932–941 (2018).
- ⁴⁸M. J. Thiecke, G. Wutz, M. Muhar, W. Tang, S. Bevan, V. Malysheva, R. Stocsits, T. Neumann, J. Zuber, P. Fraser, S. Schoenfelder, J.-M. Peters, and M. Spivakov, "Cohesin-dependent and -independent mechanisms mediate chromosomal contacts between promoters and enhancers," *Cell Rep.* **32**, 107929 (2020).
- ⁴⁹L. Calderon, F. D. Weiss, J. A. Beagan, M. S. Oliveira, R. Georgieva, Y.-F. Wang, T. S. Carroll, G. Dharmalingam, W. Gong, K. Tossell, V. de Paola, C. Whilding, M. A. Ungless, A. G. Fisher, J. E. Phillips-Cremins, and M. Merkenschlager,

- "Cohesin-dependence of neuronal gene expression relates to chromatin loop length," *eLife* **11**, e76539 (2022).
- ⁵⁰L. Kane, I. Williamson, I. M. Flyamer, Y. Kumar, R. E. Hill, L. A. Lettice, and W. A. Bickmore, "Cohesin is required for long-range enhancer action at the *Shh* locus," *Nat. Struct. Mol. Biol.* **29**, 891–897 (2022).
- ⁵¹N. J. Rinzema, K. Sofiadis, S. J. D. Tjalsma, M. J. A. M. Versteegen, Y. Oz, C. Valdes-Quezada, A.-K. Felder, T. Filipovska, S. van der Elst, Z. de Andrade dos Ramos, R. Han, P. H. L. Krijger, and W. de Laat, "Building regulatory landscapes reveals that an enhancer can recruit cohesin to create contact domains, engage CTCF sites and activate distant genes," *Nat. Struct. Mol. Biol.* **29**, 563–574 (2022).
- ⁵²T.-H. S. Hsieh, C. Cattoglio, E. Slobodyanyuk, A. S. Hansen, X. Darzacq, and R. Tjian, "Enhancer-promoter interactions and transcription are largely maintained upon acute loss of CTCF, cohesin, WAPL or YY1," *Nat. Genet.* **54**, 1919–1932 (2022).
- ⁵³A. Aljahani, P. Hua, M. A. Karpinska, K. Quililan, J. O. J. Davies, and A. M. Oudelaar, "Analysis of sub-kilobase chromatin topology reveals nanoscale regulatory interactions with variable dependence on cohesin and CTCF," *Nat. Commun.* **13**, 2139 (2022).
- ⁵⁴V. Y. Goel, M. K. Huseyin, and A. S. Hansen, "Region capture micro-C reveals coalescence of enhancers and promoters into nested microcompartments," *Nat. Genet.* **55**, 1048–1056 (2023).
- ⁵⁵W. Bialek, T. Gregor, and G. Tkačik, "Action at a distance in transcriptional regulation," *arXiv*, 1912.08579 (2019).
- ⁵⁶H. B. Brandão, M. Gabriele, and A. S. Hansen, "Tracking and interpreting long-range chromatin interactions with super-resolution live-cell imaging," *Curr. Opin. Cell Biol. Cell Nucl.* **70**, 18–26 (2021).
- ⁵⁷M.-T. Wei, Y.-C. Chang, S. F. Shimobayashi, Y. Shin, A. R. Strom, and C. P. Brangwynne, "Nucleated transcriptional condensates amplify gene expression," *Nat. Cell Biol.* **22**, 1187–1196 (2020).
- ⁵⁸K. Monfils and T. S. Barakat, "Models behind the mystery of establishing enhancer-promoter interactions," *Eur. J. Cell Biol.* **100**, 151170 (2021).
- ⁵⁹M. Gabriele, H. B. Brandão, S. Grosse-Holz, A. Jha, G. M. Dailey, C. Cattoglio, T.-H. S. Hsieh, L. Mirny, C. Zechner, and A. S. Hansen, "Dynamics of CTCF- and cohesin-mediated chromatin looping revealed by live-cell imaging," *Science* **376**, 496–501 (2022).
- ⁶⁰J. Li, Y. Liu, H. Rhee, S. Ghosh, L. Bai, B. Pugh, and D. Gilmour, "Kinetic competition between elongation rate and binding of NELF controls promoter-proximal pausing," *Mol. Cell* **50**, 711–722 (2013).
- ⁶¹K. Adelman and J. T. Lis, "Promoter-proximal pausing of RNA polymerase II: Emerging roles in metazoans," *Nat. Rev. Genet.* **13**, 720–731 (2012).
- ⁶²L. Core and K. Adelman, "Promoter-proximal pausing of RNA polymerase II: A nexus of gene regulation," *Genes Dev.* **33**, 960–982 (2019).
- ⁶³P. Natarajan, K. Shrinivas, and A. K. Chakraborty, "A model for cis-regulation of transcriptional condensates and gene expression by proximal lncRNAs," *Biophys. J.* **122**, 2757–2772 (2023).
- ⁶⁴M. Doi and S. F. Edwards, *The Theory of Polymer Dynamics, International Series of Monographs on Physics* (Oxford University Press, 1986), Vol. 73.
- ⁶⁵V. I. P. Keizer, S. Grosse-Holz, M. Woringer, L. Zambon, K. Aizel, M. Bongaerts, F. Delille, L. Kolar-Znika, V. F. Scolari, S. Hoffmann, E. J. Banigan, L. A. Mirny, M. Dahan, D. Fachinetti, and A. Coulon, "Live-cell micromanipulation of a genomic locus reveals interphase chromatin mechanics," *Science* **377**, 489–495 (2022).
- ⁶⁶M. Socol, R. Wang, D. Jost, P. Carrivain, C. Vaillant, E. Le Cam, V. Dahirel, C. Normand, K. Bystricky, J.-M. Victor, O. Gadal, and A. Bancaud, "Rouse model with transient intramolecular contacts on a timescale of seconds recapitulates folding and fluctuation of yeast chromosomes," *Nucleic Acids Res.* **47**, 6195–6207 (2019).
- ⁶⁷K. E. Polovnikov, H. B. Brandão, S. Belan, B. Slavov, M. Imakaev, and L. A. Mirny, "Crumpled polymer with loops recapitulates key features of chromosome organization," *Phys. Rev. X* **13**, 041029 (2023).
- ⁶⁸P. Mach, P. I. Kos, Y. Zhan, J. Cramard, S. Gaudin, J. Tünnermann, E. Marchi, J. Eglinger, J. Zuin, M. Kryzhanovska, S. Smallwood, L. Gelman, G. Roth, E. P. Nora, G. Tiana, and L. Giorgietti, "Cohesin and CTCF control the dynamics of chromosome folding," *Nat. Genet.* **54**, 1907–1918 (2022).
- ⁶⁹B. Beltran, D. Kannan, Q. MacPherson, and A. J. Spakowitz, "Geometrical heterogeneity dominates thermal fluctuations in facilitating chromatin contacts," *Phys. Rev. Lett.* **123**, 208103 (2019).
- ⁷⁰A. Lesage, V. Dahirel, J.-M. Victor, and M. Barbi, "Polymer coil-globule phase transition is a universal folding principle of Drosophila epigenetic domains," *Epigenet. Chromatin* **12**, 28 (2019).
- ⁷¹A. Goychuk, D. Kannan, A. K. Chakraborty, and M. Kardar, "Polymer folding through active processes recreates features of genome organization," *Proc. Natl. Acad. Sci. U. S. A.* **120**, e2221726120 (2023).
- ⁷²T. Muramoto, D. Cannon, M. Gierliński, A. Corrigan, G. J. Barton, and J. R. Chubb, "Live imaging of nascent RNA dynamics reveals distinct types of transcriptional pulse regulation," *Proc. Natl. Acad. Sci. U. S. A.* **109**, 7350–7355 (2012).
- ⁷³M. E. Pownall, L. Miao, C. E. Vejnar, O. M'Saad, A. Sherrard, M. A. Frederick, M. D. J. Benitez, C. W. Boswell, K. S. Zaret, J. Bewersdorf, and A. J. Giraldez, "Chromatin expansion microscopy reveals nanoscale organization of transcription and chromatin," *Science* **381**, 92–100 (2023).
- ⁷⁴S. Marbach, H. Yoshida, and L. Bocquet, "Local and global force balance for diffusiophoretic transport," *J. Fluid Mech.* **892**, A6 (2020).
- ⁷⁵T.-K. Kim, M. Hemberg, J. M. Gray, A. M. Costa, D. M. Bear, J. Wu, D. A. Harmin, M. Laptev, K. Barbara-Haley, S. Kuersten, E. Markenscoff-Papadimitriou, D. Kuhl, H. Bito, P. F. Worley, G. Kreiman, and M. E. Greenberg, "Widespread transcription at neuronal activity-regulated enhancers," *Nature* **465**, 182–187 (2010).
- ⁷⁶S. Ramasamy, A. Aljahani, M. A. Karpinska, T. B. N. Cao, T. Velychko, J. N. Cruz, M. Lidschreiber, and A. M. Oudelaar, "The Mediator complex regulates enhancer-promoter interactions," *Nat. Struct. Mol. Biol.* **30**, 991–1000 (2023).
- ⁷⁷N. T. Crump, E. Ballabio, L. Godfrey, R. Thorne, E. Repapi, J. Kerry, M. Tapia, P. Hua, C. Lagerholm, P. Filippakopoulos, J. O. J. Davies, and T. A. Milne, "BET inhibition disrupts transcription but retains enhancer-promoter contact," *Nat. Commun.* **12**, 223 (2021).
- ⁷⁸T. Yamamoto, T. Sakauye, and H. Schiessel, "Slow chromatin dynamics enhances promoter accessibility to transcriptional condensates," *Nucleic Acids Res.* **49**, 5017–5027 (2021).
- ⁷⁹H. Chen, M. Levo, L. Barinov, M. Fujioka, J. B. Jaynes, and T. Gregor, "Dynamic interplay between enhancer-promoter topology and gene activity," *Nat. Genet.* **50**, 1296–1303 (2018).
- ⁸⁰J. M. Alexander, J. Guan, B. Li, L. Maliskova, M. Song, Y. Shen, B. Huang, S. Lomvardas, and O. D. Weiner, "Live-cell imaging reveals enhancer-dependent Sox2 transcription in the absence of enhancer proximity," *eLife* **8**, e41769 (2019).
- ⁸¹D. B. Brückner, H. Chen, L. Barinov, B. Zoller, and T. Gregor, "Stochastic motion and transcriptional dynamics of pairs of distal DNA loci on a compacted chromosome," *Science* **380**, 1357–1362 (2023).
- ⁸²J. Y. Xiao, A. Hafner, and A. N. Boettiger, "How subtle changes in 3D structure can create large changes in transcription," *eLife* **10**, e64320 (2021).
- ⁸³A. M. Chiariello, F. Corberi, and M. Salerno, "The interplay between phase separation and gene-enhancer communication: A theoretical study," *Biophys. J.* **119**, 873–883 (2020); *arXiv:2010.07681*.
- ⁸⁴T. Quail, S. Golfier, M. Elsner, K. Ishihara, V. Murugesan, R. Renger, F. Jülicher, and J. Brugués, "Force generation by protein-DNA co-condensation," *Nat. Phys.* **17**, 1007–1012 (2021).
- ⁸⁵Y. Shin, Y.-C. Chang, D. S. W. Lee, J. Berry, D. W. Sanders, P. Ronceray, N. S. Wingreen, M. Haataja, and C. P. Brangwynne, "Liquid nuclear condensates mechanically sense and restructure the genome," *Cell* **175**, 1481–1491.e13 (2018).
- ⁸⁶A. R. Strom, Y. Kim, H. Zhao, Y.-C. Chang, N. D. Orlovsky, A. Košmrlj, C. Storm, and C. P. Brangwynne, "Condensate interfacial forces reposition DNA loci and probe chromatin viscoelasticity," *Cell* **187**, 5282–5297.e20 (2024).
- ⁸⁷Q. Zhang, H. Shi, and Z. Zhang, "Dynamic kissing model for enhancer-promoter communication on the surface of transcriptional condensates," *Phys. Rev. E* **111**, 054402 (2025).
- ⁸⁸M. Stortz, D. M. Presman, and V. Levi, "Transcriptional condensates: A blessing or a curse for gene regulation?," *Commun. Biol.* **7**, 187 (2024).